http://dx.doi.org/10.5012/bkcs.2012.33.1.243

Synthesis and High Photocatalytic Activity of Zn-doped TiO_2 Nanoparticles by Sol-gel and Ammonia-Evaporation Method

Thanh Binh Nguyen, Moon-Jin Hwang,† and Kwang-Sun Ryu*

*Department of Chemistry, University of Ulsan, Ulsan 680-749, Korea. *E-mail: ryuks@ulsan.ac.kr*
†Energy Harvest-Storage Research Center, University of Ulsan, Ulsan 680-749, Korea
Received August 13, 2011, Accepted November 22, 2011

Photocatalysis has been applied to decompose the waste and toxic materials produced in daily life and in the global environment. Pure TiO_2 (Zn-TiO_2-0) and Zn-doped TiO_2 (Zn-TiO_2-x, x = 3-10 mol %) samples were synthesized using a novel sol-gel and ammonia-evaporation method. The Zn-doped TiO_2 samples showed high photocatalytic activity for the degradation of methylene blue (MB). The physicochemical properties of the samples were investigated using XRD, SEM, ICP, DLS and BET methods. In addition, the most important measurement of photocatalytic ability was investigated by a UV-vis spectrophotometer. The effects of the mol % of zinc ion doping in TiO_2 on photocatalytic activity were studied. Among the mol % Zn ions investigated, the Zn-TiO_2-9 sample showed the highest photoreactivity. This sample removed 91.4% of the MB after 4 h, while the pure TiO_2 only removed 46.4% of the MB.

Key Words : Zn-doped TiO_2, Photoreactivity, Degradation, Methylene blue

Introduction

In recent years, the use of TiO_2 nanoparticles as a photocatalyst has been extensively studied in order to decompose various kinds of organic pollutants because of their high oxidative power, non-toxicity, photostability, and water insoluble properties under most conditions.[1-7] However, the photocatalytic activity of TiO_2 is limited to its irradiation wavelength in the UV region; therefore, the effective utilization of solar energy is limited to about 3-5% of the total solar spectrum.[1-5] The photoreactivity of semiconductor materials must be able to be controlled by three basic parameters: (i) the light absorption property, (ii) the rates of reduction and oxidation of the reaction substrate by electron (e^-) and hole (h^+), respectively, and (iii) the rate of e^- and h^+ recombination.

TiO_2 photocatalytic activity has been improved by doping the transition metal ions used in its formation, such as Fe^{2+}, Mn^{2+}, Cu^{2+}, Zn^{2+}, etc. Zn-doped TiO_2 has proven to be an effective mechanism for photocatalysis because of its corrosion, hardness, semiconductor and magnetic properties, good transparency, and electron mobility. Moreover, the separation rate of the photoinduced charge was shown to be increased when zinc ions were used because of the difference in the energy band positions. In addition, Zn^{2+} reacts with dye molecules.[6,10] Therefore, the effects of Zn-doped TiO_2 are very important.

Several previous methods have been used, such as the sol-gel method,[4-6,14] flame method,[13] and ball milling.[2] In this paper, Zn-doped TiO_2 nanoparticles with high photocatalytic activity were synthesized by a sol-gel and ammonia-evaporation method at low temperature. We used the sol-gel method because it allows very simple control of particle size and the experimental process. In addition, the ammonia-evaporation method also can control both the precipitation and the passivation of crystal surfaces.[11-13] The combination of these methods fosters the generation of a stable structure between the TiO_2 and ZnO.

Experimental Method

Chemicals. The titanium (IV) isopropoxide (TTIP, 97%) and isopropanol (IPA, > 99.8%) used were obtained from Sigma-Aldrich. The zinc sulfate heptahydrate ($ZnSO_4 \cdot 7H_2O$, > 99.0%) and ammonium hydroxide (NH_4OH, 25-28%) were made by Dae Jung Chemicals. The TTIP and $ZnSO_4 \cdot 7H_2O$ were used as the precursors for the TiO_2 and Zn components, respectively, and distilled water was used as the solvent.

Preparation of TiO_2 and Zn-doped TiO_2 Nanoparticles. The zinc sulfate heptahydrate was dissolved in distilled water to a final 0.2 M until the solution became homogeneous. All samples are designated as Zn-TiO_2-x, where x is the mol % of the Zn (x = 0, 3, 5, 7, 9, and 10). The Zn-TiO_2-x samples were prepared as shown in Scheme 1. The A and B solutions were prepared so that the molar ratio of TTIP, IPA, and H_2O was 1:5:100. Moreover, the influence of the initial concentration of the zinc solution (y = 0.2, 0.1, and 0.05 M) on the photocatalytic activity at the optimal mol % of Zn was investigated with samples named Zn-TiO_2-x-y.

Characterization. The crystalline phase was determined using X-ray diffraction (XRD, Cu K_α radiation, 40 kV, 100 mA, λ = 1.54059 Å, Ultra-X, Rigaku Co., Japan) at a step scan rate of 0.02°/0.3 s in the 2θ range of 10-80°. The X-ray wavelength, the full width at half maximum (FWHM) of the diffraction line, and the diffraction angle were measured by MDI/JADE 7 software. The morphology and the composition of the samples were analyzed using scanning electron

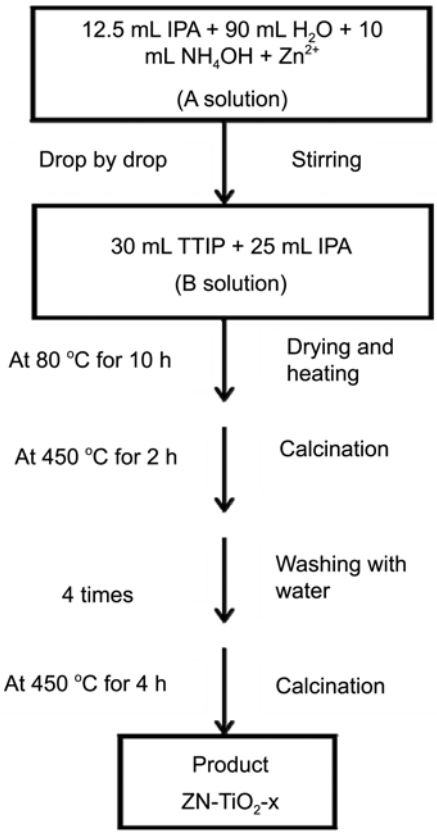

Scheme 1. Synthesis of Zn-doped TiO_2.

microscopy (SEM, Supra 40, Carl Zeiss Co., Ltd., Germany). A Zetasizer Nano Series instrument (Nano ZS, Malvern Instruments Ltd.) was used for measuring the particle size distribution (PSD) by dynamic light scattering (DLS) method. An inductively coupled plasma optical emission spectrometer (iCAP 6500, Thermo Electron Corporation) was used for measuring the weight ratio of the Zn and Ti. The surface area was measured by BET analysis (nanoPOROSITY-XQ, Mirae Scientific Instruments Co., Korea).

Photocatalytic Activity Evaluation. Methylene blue ($C_{16}H_{18}N_3SCl$, MB) is a common chemical material in the chemical and biological industries. Therefore, it was chosen as a model pollutant. The photocatalytic activity of the Zn-doped TiO_2 nanoparticles was evaluated by measuring the decomposition of an aqueous methylene blue ($C_0 = 1 \times 10^{-5}$ M) solution. After adsorption for 20 min in the dark, four surrounding 20 W black-light blue lamps (λ_{max} = 352 nm, 0.16 A) were activated, and 3.5 mL samples were withdrawn at different time intervals over 240 min and placed into different syringes and filters. The MB concentration was characterized by a UV-vis spectrophotometer (OPTIZEN POP, Mecasys Co., Ltd., Korea) at λ_{max} = 666 nm, and the residual percentages of MB were calculated using the equation:

$$MB = \frac{C}{C_0} \times 100\ (\%) \qquad (1)$$

where C_0 and C are the initial concentration of MB and the concentration at the irradiation time, respectively.

Figure 1. The colors of the Zn-TiO_2-x samples.

Results and Discussion

The colors of the Zn-TiO_2-x samples are shown in Figure 1. When the mol % of the Zn doping was increased, the color of the samples changed from light yellow (pure TiO_2) to white. The white sample color has an advantage for the photoreaction process because the sample is more transparent to allow light to enter into the product. Moreover, the existence of zinc ions was confirmed by measuring the weight ratios of Zn and Ti, as shown in Table 1. For example, the Ti/Zn ratios are 53.5/1.0 and 49.1/4.2 for the Zn-TiO_2-3 and Zn-TiO_2-10 samples, respectively. The Ti/Zn ratio indicated that the actual amount of reacted Zn was from 45 to 59% of the Zn design amount.

In Figure 2, the XRD patterns of the Zn-TiO_2-x samples were similar. All phases of the samples exhibited anatase phase diffraction peaks and no characteristic peak of zinc metal or oxides, which implies that the zinc ions incorporated into the lattice of the anatase TiO_2 or zinc oxide were small and highly dispersed.[6] However, the pure TiO_2 sample and Zn-doped TiO_2 samples at the (101) plane produced slightly shifted peaks, as shown in Table 1. The crystallite size of the samples was calculated following Scherrer's equation;[4]

$$D = \frac{k\lambda}{\beta \cos\theta} \qquad (2)$$

where D is the crystallite size, k is a constant (shape factor, about 0.9), λ is the X-ray wavelength (0.154059 nm), β is the full width at half maximum (FWHM) of the diffraction

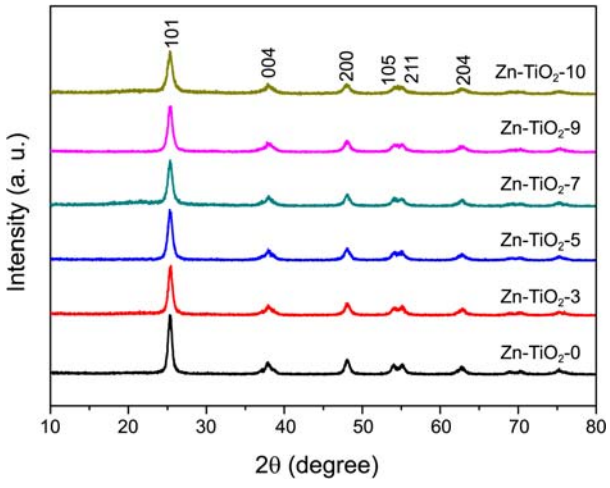

Figure 2. X-ray diffraction patterns of the Zn-TiO_2-x samples.

Table 1. Physicochemical properties of the Zn-TiO_2-x samples

Sample	2θ (°)	d-spacing (Å)	Crystallite size (nm)	Average size (d. nm)	S_{BET} (m^2/g)	Average pore diameter (nm)	ICP Ti/Zn
Zn-TiO_2-0	25.3	3.5174	15.08	576	81.32	5.73	-
Zn-TiO_2-3	25.439	3.4985	14.78	1180	87.21	6.02	53.5/1.0
Zn-TiO_2-5	25.3	3.5714	13.48	721	89.77	5.49	54.7/1.86
Zn-TiO_2-7	25.359	3.5093	13.62	678	94.52	6.39	53.3/3.72
Zn-TiO_2-9	25.4	3.5038	13.59	757	83.11	4.94	49.8/3.87
Zn-TiO_2-10	25.32	3.5147	14.03	1908	101.27	4.92	49.1/4.2

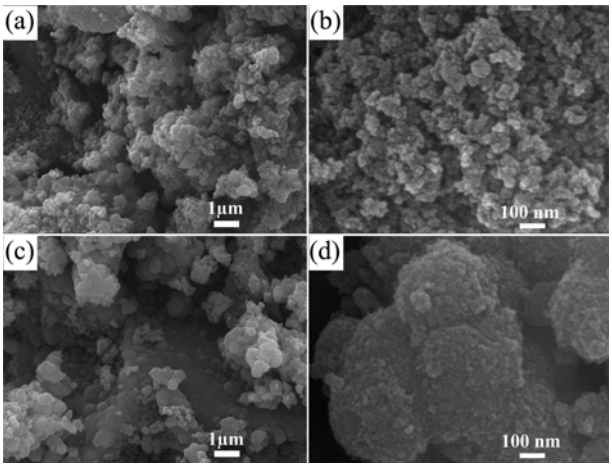

Figure 3. SEM images of the Zn-TiO_2-x samples. (a, b) Zn-TiO_2-0; (c, d) Zn-TiO_2-10.

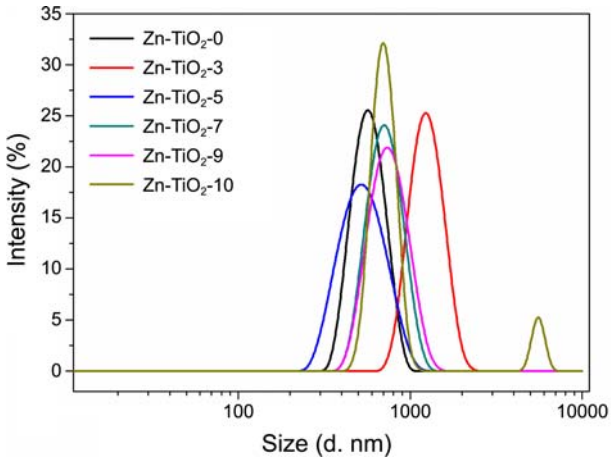

Figure 4. Particle size distributions of the Zn-TiO_2-x samples.

line, and θ is the diffraction angle. When the mol % of the zinc ion doping in TiO_2 was increased, the crystallite size decreased. The particle sizes in the samples were in the range of 13.5-15.1 nm.

The morphology of the sample is shown in Figure 3. The particle size of the sample is about 15 nm. The sizes of the particles and the surfaces of the samples did not differ significantly so the SEM images of the pure TiO_2 and the Zn-TiO_2-10 are shown. When the amount of Zn doping was increased, the surface of the sample was the agglomeration. All of the samples used the same amount of ammonium at a controlled pH in the reaction. Therefore, when the amount of Zn doping was increased, the pH decreased because the ammonium was diluted due to the additional water in the zinc solution. This indicates that the repulsion of TiO_6 units decreased, resulting in a large, agglomerated particles network. However, the network of the particle affects not only the pH, but also the amount of water. By increasing the Zn doping, the total amount of water in the reaction increased, so the space needed for $[TiO_6]^{n+}$ unit adjustment is larger. Therefore, the arrangement of the units will be more regular when the amount of water was increased.[15] When comparing the two factors (pH and water) on network and agglomeration, the effect of pH is greater than that of the water content.

The particle size distributions and the average diameter of the Zn-doped TiO_2 samples were shown in Figure 4 and Table 1. The average diameter of the Zn-TiO_2-x (x = 3-10) increased with increasing Zn mol % in TiO_2. Therefore, the samples contain large particle or aggregate. According to SEM images, the samples have an aggregated form because the samples were synthesized at low temperature (80 °C). Average diameter of the pure TiO_2 is 576 nm while that of other samples range from 678 to 1908 nm. When the amount of Zn doping was reached to 10 mol %, the dispersity became heterogeneous and the particle size increased remarkably.

The nitrogen adsorption-desorption isotherms of the Zn-doped TiO_2 are shown in Figure 5. All isotherms were

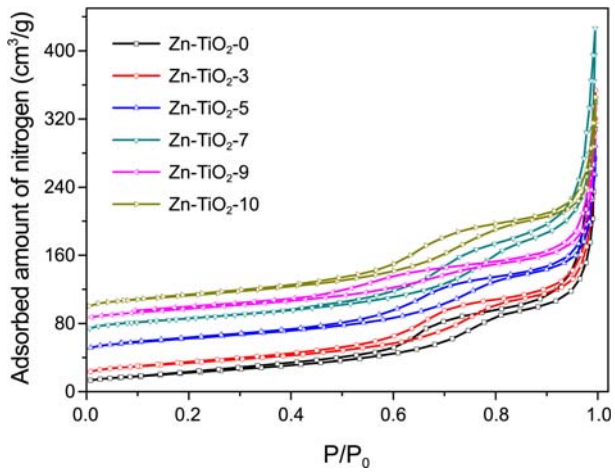

Figure 5. N_2 adsorption-desorption isotherm of the Zn-TiO_2-x samples.

identified as type IV according to the IUPAC classification, where the pore sizes are similar to those of the mesoporous family (radius from 2-50 nm). All of the samples had hysteresis loops, which were identified as type H3 and indicate the existence of slit-shape pore channels. The hysteresis loop included two areas: the first includes P/P_0 values between 0.3 and 0.7, indicating textural mesoporosity, and the second contains P/P_0 values greater than 0.7, in which the particles create a pore framework. When the Zn ions were doped in TiO_2, the framework was reduced, especially the Zn-TiO_2-x (x = 9, 10), because the particle sizes were reduced and agglomerated. The specific surface area (S_{BET}) was calculated from the linear BET plot (P/P_0 range of 0.06-0.2), the total pore volume was measured using the BJH method at $P/P_0 = 0.99$,[9] and the average pore diameter was determined using the BJH formula and adsorption isotherm. These results are summarized in Table 1. The S_{BET} of the sample depends on the crystallite size, crystallite phase, pore size, and shape.[9] Therefore, the S_{BET} of the samples increased regularly along with increasing Zn doping, except for that of the Zn-TiO_2-9 sample, such as increasing S_{BET} from 81.3 to 101.3 m^2/g, which is the advantage of photocatalysis.

Photocatalyst Test. The photocatalytic activity is shown in Figure 6 according to the percentage of residual MB ($C/C_0 \times 100$). For pure TiO_2 (x = 0) after 4 h, the percentage of residual MB was 53.7%. When the mol % of the zinc ions doped in TiO_2 was increased, the photocatalytic activity increased, and the value of the $C/C_0 \times 100$ was reduced accordingly. Most significantly, for the Zn-TiO_2-9 sample, the percentage of the residual MB was only 8.6%. The Zn-doped TiO_2 was significantly promoted in the photocatalyst. The effect of Zn doping on the photocatalytic activity was reflected in the crystalline size and S_{BET}, which directly affect the photoreactivity.

Effect of Zn Doping on Energy Level. The A solution includes ammonium and zinc ions. Therefore, a precipitate was formed according to the reaction described in (3)-(6):

$$ZnSO_4 + 2NH_4OH \rightarrow Zn(OH)_2 + (NH_4)_2SO_4 \quad (3)$$

$$Zn(OH)_2 + 4NH_4OH \rightarrow Zn(NH_3)_4(OH)_2 + 4H_2O \quad (4)$$

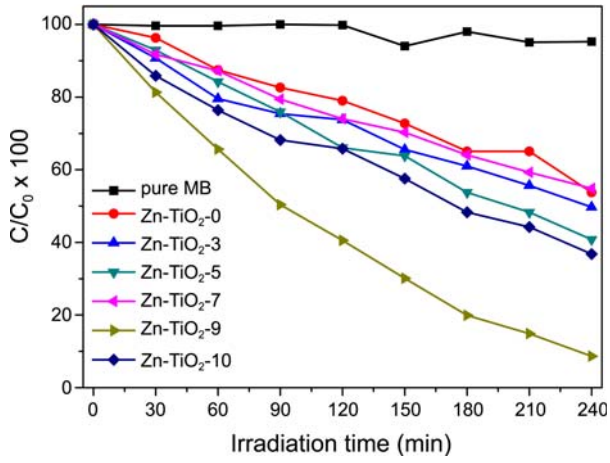

Figure 6. The effect of zinc content on photocatalytic activity.

$$Zn(NH_3)_4(OH)_2 \rightarrow Zn(NH_3)_4^{2+} + 2OH^- \quad (5)$$

$$Zn(NH_3)_4^{2+} + 2OH^- \rightarrow ZnO + 4NH_3 + H_2O \quad (6)$$

The structure of TiO_2 in sol-gel contains many hydroxyl groups, which are used by both Ti and Zn. When the solution was heated above 80 °C, ZnO formed, so the structure of TiO_2 and ZnO particles took form that they make structure with hydroxyl groups together. Therefore, the band gap of the Zn-doped TiO_2 changed.

Metal ion (Zn^{2+}) dopants influenced the photoreactivity of the TiO_2 by acting as electron or hole traps and by altering the e^-/h^+ pair recombination rate through the following process:

$$M^{n+} + e_{cb}^- \rightarrow M^{(n-1)+} \quad \text{electron trap} \quad (7)$$

$$M^{n+} + h_{vb}^+ \rightarrow M^{(n+1)+} \quad \text{hole trap} \quad (8)$$

The dimensions of the semiconductor can be on the order of nanometers and the energy shifts according to the quantum size effect. The shift of the conduction band (CB) may accelerate the reduction ($E_M{}^{n+}/M^{(n-1)+} < E_{cb}$), while that of the valance band (VB) may increase the oxidation reaction ($E_M{}^{n+}/M^{(n+1)+} < E_{vb}$). Therefore, the band gap energy of the Zn-doped TiO_2 samples is extremely small compared with that of pure TiO_2.

Effect of Recombination on Photocatalytic Activity. The photocatalytic reaction occurs at the surface of a semiconductor. Therefore, an increase in the surface area and a reduction in the particle size cause an increase in the photoactivity. For the Zn-TiO_2-9 sample, the crystalline size was 13.59 nm, which is only larger than that of the Zn-TiO_2-5 sample. However, the S_{BET} of the Zn-TiO_2-9 sample was the smallest (83.11 m^2/g), which is a disadvantage with regard to photocatalytic activity. From the results of the photocatalyst test, the Zn-TiO_2-9 sample demonstrated the optimum performance. Hence, the rate of recombination affects the photocatalytic reaction more than does the specific surface area. The recombination process can be performed *via* volume recombination or surface recombination.[6-8] Volume recombination is the dominant process in large semiconductor particles. The Zn-TiO_2-9 sample had a small particle size, so the recombination rate was reduced. On the other hand, the recombination was affected by the defect factors, for example, those of the Ti^{3+} and Zn ions. However, defects can reduce or increase the recombination time. Therefore, an optimal doping mol % of the Zn ions is necessary in order to reduce the maximum recombination rate.

Influence of Initial Concentration of $ZnSO_4$ on Photocatalytic Activity. Nine mol % of Zn is the best for the synthesis of Zn-TiO_2-x by the sol-gel and ammonia-evaporation method. Ammonia controls both the precipitation and the passivation of the crystal surface. The pH controls the charges carried by the particles, while the ammonia molecules can passivate throughout the surface and thereby influence the growth and aggregation behaviors of the particles.[11] In addition, the initial concentration of the $ZnSO_4$ affects not only the pH, but also the total amount of water in

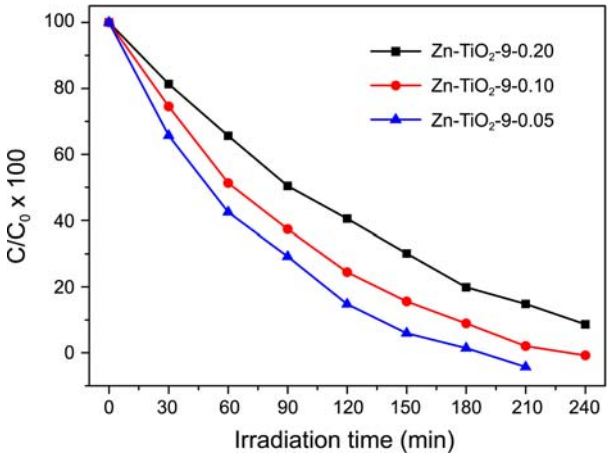

Figure 7. The effect of initial concentration of $ZnSO_4$ on photocatalytic activity.

the reaction. Two factors (the pH and the amount of water) directly affect the efficiency of the photocatalytic reaction. The effect of the initial concentration of the $ZnSO_4$ on the photocatalytic activity is shown in Figure 7. For the initial concentration of the $ZnSO_4$ with 0.20 M, MB was reduced by 1.4% after 4 h. By reducing the initial concentration, the MB was removed quickly. For instance, for 0.1 M $ZnSO_4$, the percentage of residual MB was 8.9% after 3 h, which is the same as that for 0.2 M $ZnSO_4$ after 4 h. The change in the initial concentration of the photoreaction took place in less than 1 h. For the 0.05 M $ZnSO_4$ after 3 h, the concentration of MB was reduced by 98.6%. After 210 min, the 0.05 M sample resulted in the complete removal of MB ($C/C_0 \times 100 = -4.3$). As shown in the results, the Zn-TiO_2-9-0.05 sample resulted in the optimal degradation of MB.

Conclusions

The mol % Zn-doped TiO_2 samples were fabricated successfully by the sol-gel and ammonia-evaporation method. The Zn-doped TiO_2 had different energy level and surface area compared to that of pure TiO_2, which increased the photocatalytic activity from 46.3 to 91.4%. Among the mol % doping amounts in the TiO_2, the Zn-TiO_2-9 sample produced the best performance, and the optimal initial concentration of $ZnSO_4$ was 0.05 M.

Acknowledgments. This work (Grants No. 00039007) was supported by Business for Academic-industrial Cooperative establishments funded Korea Small and Medium Business Administration in 2011 and by the Priority Research Centers Program through the National Research Foundation of Korea (NRF) funded by the Ministry of Education, Science and Technology (2009-0093818).

References

1. Kaneko, M.; Okura, I. Photocatalysis: science and technology: Kadansha and Springer: Japan, 2002.
2. Chen, S.; Zhao, W.; Liu, W.; Zhang, S. *Appl. Sur. Sci.* **2008**, *255*, 2478.
3. Zhao, Y.; Li, C.; Liu, X.; Gu, F.; Du, H. L.; Shi, L. *Appl. Catal. B: Environ.* **2008**, *79*, 208.
4. Yu, H. F.; Zhang, Z. W.; Hu, F. C. *J. Alloy Compd.* **2008**, *465*, 484.
5. Österlund, L.; Štengl, V.; Mattsson, A.; Bakardjieva, S.; Andersson, P. O.; Opluštil, F. J. *Appl. Catal. B: Environ.* **2009**, *88*, 194.
6. Devi, L. G.; Murthy, B. N.; Kumar, S. G. *Mater. Sci. Eng. B* **2010**, *166*, 1.
7. Zhang, Z.; Wang, C. C.; Zakaria, R.; Ying, J. Y. *J. Phys. Chem. B* **1998**, *102*, 10871.
8. Choi, W.; Termin, A.; Hoffmann, M. R. *J. Phys. Chem.* **1994**, *98*, 13669.
9. Lowell, S.; Shields, J. E. Powder surface area and porosity: Chapman and Hall, London, 1991.
10. Zhiyong, Y.; Bensimon, M.; Sarria, V.; Stolitchnov, I.; Jardim, W.; Laub, D.; Mielczarski, E.; Mielczarski, J.; Minsker, L. K.; Kiwi, J. *Appl. Catal. B: Environ.* **2007**, *76*, 185.
11. Li, Y.; Tan, B.; Wu, Y. *Chem. Mater.* **2007**, *20*, 567.
12. Chaudhuri, T. K.; Kothari, A. *Journal of Optoelectronic and Biomedical Materials* **2009**, *1*, 20.
13. Tian, J.; Wang, J.; Dai, J.; Wang, X.; Yin, Y. *Surf. Coating Tech.* **2009**, *204*, 723.
14. Liao, S.; Donggen, H.; Yu, D.; Su, Y.; Yuan, G. *J. Photochem. Photobiol. Chem.* **2004**, *168*, 7.
15. Chen, Z.; Zhao, G.; Li, H.; Han, G.; Song, B. *J. Am. Ceram. Soc.* **2009**, *92*, 1024.